Evaluation of the effect of rolling correction of double-o-tunnel shields via one-side loading

Shui-Long Shen, Yan-Jun Du, and Chun-Yong Luo

Abstract: During construction of a double-o-tunnel (DOT), rolling will inevitably occur due to the following: (*i*) nonuniformity of subsoil condition, (*ii*) manufacturing errors in the DOT shield machine, (*iii*) different pulling forces at two sides of the DOT, (*iv*) effect of assembled segments, (*v*) loss of grout, and (*vi*) inappropriate operation. In engineering practice, rolling correction using a one-side load at the elevated side is a cost-effective method. The weight of the one-side load is determined by the experience of the engineers and (or) through observation of the returned rolling angle. However, these methods cannot predict the value of the one-side load before applying it. This paper presents a series of finite element analyses that was performed to investigate the relationship among the one-side load, rolling angle, and subsoil deformation. The analytical results show that the proposed approach can predict field-observed data well. It is concluded that analytical results can be used as guidance for DOT construction.

Key words: double-o-tunnel (DOT) shield, rolling correction, one-side loading, finite element analysis, settlement.

Résumé : Pendant la construction d'un tunnel double circulaire (« double-o-tunnel, DOT »), il y aura inévitablement du roulage pour les raisons suivantes : (*i*) des conditions de sous-sol non uniformes; (*ii*) des erreurs lors de la manufacture du bouclier pour foncer le tunnel DOT; (*iii*) des forces différentes tirant de chaque côté du tunnel DOT; (*iv*) les effets des segments assemblés; (*v*) les pertes de coulis; (*vi*) une opération inappropriée. Dans la pratique, une méthode efficace et peu coûteuse est la correction du roulage par l'ajout d'une charge d'un côté, du côté élevé. Le poids de la charge est déterminé par l'expérience des ingénieurs et (ou) par l'observation de l'angle de roulage suite à l'application de la charge d'un côté. Cependant, ces méthodes ne peuvent pas prédire la valeur de la charge avant son application. Cet article présente des analyses par éléments finis qui ont été effectuées pour évaluer la relation entre la charge d'un côté, l'angle de roulage et la déformation du sous-sol. Les résultats analytiques démontrent que l'approche proposée permet de bien prédire les observations sur le terrain. On peut ainsi conclure que les résultats analytiques peuvent être utilisés pour diriger la construction d'un DOT.

Mots-clés : bouclier pour le fonçage d'un tunnel double circulaire (« DOT »), correction du roulage, charge d'un côté, analyse par éléments finis, tassement.

[Traduit par la Rédaction]

Introduction

The process of urbanization continuously exploits underground space in urban areas. The shield tunneling method is one of the main construction methods for urban tunnels. Generally, a shield tunnel is in a single circular configuration. However, there are many disadvantages to a single circular shield tunnel, e.g., (*i*) use of a large underground space, (*ii*) high construction costs, and (*iii*) a long construction period. To overcome these disadvantages, a new method named the double-o-tube shield tunnel (hereafter called double-o-tunnel and labeled DOT) method was proposed in Japan in the early 1980s (RANSTT 1998). DOT technology was first applied in a tunnel project in Hiroshima, Japan, in 1989 (Iida and Sumida 1992). Figure 1 illustrates the schematic configuration of a typical DOT shield; which is composed of three bodies: (*i*) head, (*ii*) middle, and (*iii*) tail. The head body includes two cutters and two soil chambers; the middle body includes two sets of cutter supporters, two sets of cutter drivers, shield jacks, and two sets of screw conveyor supporters; and the tail body includes two sets of lining assembling devices and two sets of tail grout devices. As shown in Fig. 1, one DOT shield can construct two tunnels simultaneously. Figure 2 depicts the cross-sectional view of lining segments.

During shield tunnel construction, surface settlement is inevitable due to ground loss (Peck 1969*a*). Peck (1969*a*) indicated that the shape of the surface settlement trough for a single circular shield tunnel was symmetrically distributed on either side of the centerline of the tunnel. However, if DOT tunneling was carried out, field-measured data show that in most cases, the surface settlement trough may not follow Peck's pattern (Yonei 2000; Bai and Ding 2008). Figure 3 shows a recorded case of the asymmetrical surface settlement trough of a DOT constructed in Tokyo (Yonei 2000). The asymmetrical distribution of the settlement trough may be due to the operation of rolling correction dur-

Received 4 September 2008. Accepted 20 February 2010. Published on the NRC Research Press Web site at cgj.nrc.ca on 28 September 2010.

S.-L. Shen[1] **and C.-Y. Luo.** School of Naval Architecture, Ocean, and Civil Engineering, Shanghai Jiao Tong University and State Key Laboratory of Ocean Engineering, Shanghai 200240, China.
Y.-J. Du. Institute of Geotechnical Engineering, Transportation College, Southeast University, Nanjing, Jiangsu 210096, China.

[1]Corresponding author (e-mail: slshen@sjtu.edu.cn).

Fig. 1. Schematic diagram of DOT shield: (*a*) cutter face and (*b*) longitudinal section. All dimensions in millimetres. 1, shield shell; 2, cutter; 3 copy cutter; 4, observation hole; 5, manhole; 6, soil chamber; 7, screw conveyor; 8, jack; 9, segment assembling device.

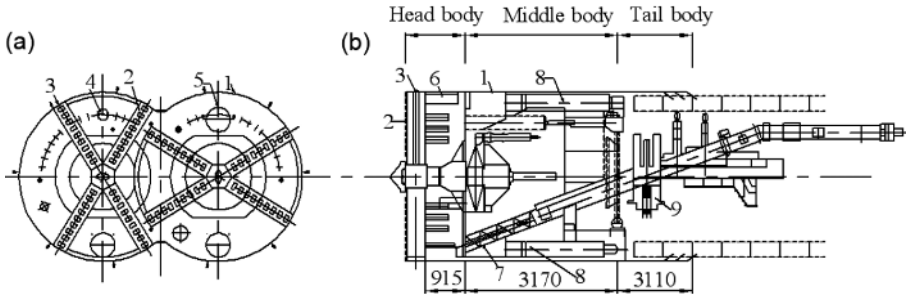

Fig. 2. Cross-sectional view of DOT and layout of segments.

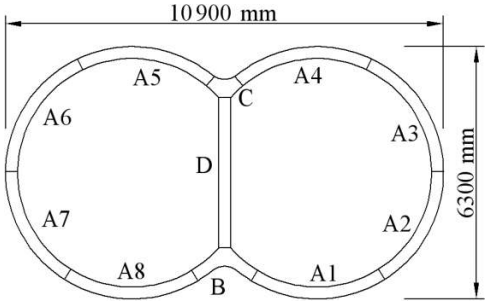

ing DOT tunneling (Iida and Sumida 1992; Yonei 2000; Ishihara et al. 2003; Shen et al. 2006, 2009).

During DOT tunneling, rolling will inevitably occur due to nonuniformity of subsoils, machine manufacturing errors, and inappropriate operation. Rolling results in different elevations of the two tunnels, and affects the life span and quality of the DOT. Therefore, rolling correction is necessary and should be conducted during shield driving (Iida and Sumida 1992; RANSTT 1998; Ishihara et al. 2003). However, rolling correction causes extra inner forces in the lining, disturbs surrounding soils, and induces additional surface settlement (Shen et al. 2009). In engineering practice, block loading on one side of the DOT shield is a cost-effective way to correct rolling (Ishihara et al. 2003). Generally, the magnitude of one-side loading is determined by the experience of the engineers and (or) through observation of the returned rolling angle. However, none of these methods can predict the value of the load before it is applied.

The objectives of this paper are to (*i*) confirm the effectiveness of the one-side loading method used to correct rolling of a DOT shield and (*ii*) evaluate the effect of one-side loading on rolling correction by finite element method (FEM) analysis.

Characteristics of DOT tunneling

Disadvantages of double-o-tunnels (DOTs)

Compared with a single circle shield tunnel, DOTs have the following characteristics:

(1) The ratio of lateral to vertical dimension for DOTs is much larger than the same ratio for circle shield tunnels, as shown in Figs. 1 and 2.

(2) DOTs have more types of segments and segment joints than circle shield tunnels. Segments in DOTs are labeled A1 to A8, B, C, and D as shown in Fig. 2.

(3) The dumbbell shape of DOTs leads to a much more complex and nonuniform distribution of internal stress in linings than that of circular shield tunnels, which consequently results in a potentially less stable lining and difficulty in lining assembly (Shen et al. 2006, 2009). Even a small tunnel rolling angle will cause considerable redistribution of internal stresses in lining segments (Shen et al. 2009).

(4) The intersected concave area between the two tunnels weakens the waterproof function during excavation (Ishihara et al. 2003; Shen et al. 2006).

(5) Subsoils can easily stick and pile up in the intersected concave area and will move together with the shield machine, which is called the "back-soil" phenomenon. This undesirable phenomenon will cause the ground to swell. After the shield passes, a large amount of ground settlement occurs (RANSTT 1998).

(6) Due to the special configuration of the DOT shield, it is difficult to control the centerline of the DOT during construction. In other words, it is difficult to control the moving trajectory of the DOT shield (Ishihara et al. 2003; Shen et al. 2006).

Moving trajectory of DOT shield

Figure 4 schematically illustrates the moving trajectory of a DOT shield during construction. The moving trajectory of the DOT shield includes rolling, yawing, and pitching. Rolling is the rotating movement of the two cross sections of the shield, yawing is the transversal right-to-left movement of the DOT shield, and pitching is the longitudinal up–down movement of the DOT shield. All these movements will lead to deviation of the tunnel centerline from the intended position. Thus, the centerline direction is controlled by these three moving states of the DOT machine during construction.

Causes of rolling

Rolling movement of a DOT shield during construction is unavoidable because of (*i*) asymmetry of the cross section of the DOT shield machine caused by manufacturing error; (*ii*) the unbalanced weight of the DOT shield machine on either side; (*iii*) different traction forces between trolleys on either side; (*iv*) different torques of the two cutters due to different soil properties and different pressures in the two soil chambers; (*v*) different earth loads due to different topography, such as slant, on either side; (*vi*) loss of real-time grouting at the tail; and (*vii*) the different supporting position of the belt conveyor for removing excavated soils. Dur-

Fig. 3. Asymmetric ground surface settlement trough induced by DOT tunneling (data from Yonei 2000).

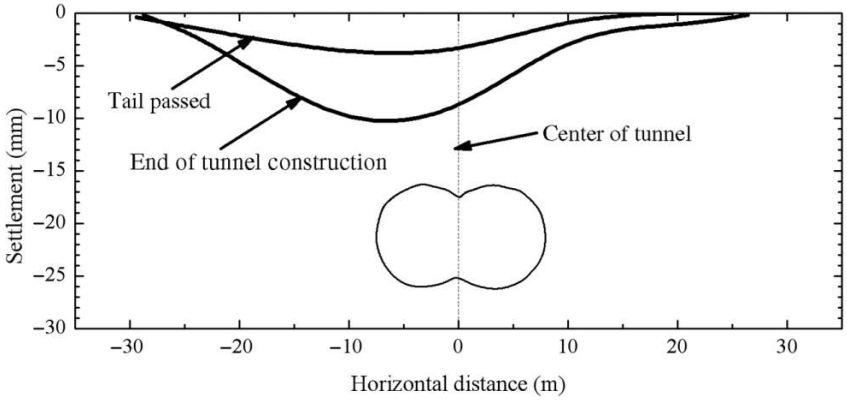

Fig. 4. Moving trajectory of DOT shield during jacking (modified after RANSTT 1998).

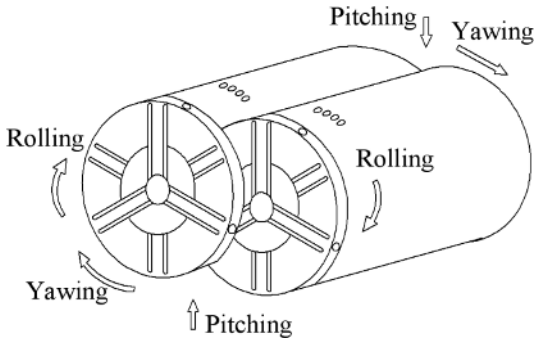

ing DOT construction, rolling occurs due to one, or a combination of several, of the aforementioned reasons (RANSTT 1998; Yonei 2000; Ishihara et al. 2003; Shen et al. 2006).

Rolling correction operation

Rolling results in different elevations between the two cross sections of the DOT and inclinations of segment D, as shown in Fig. 2. Thus, higher stress levels may occur in rolled DOT linings than those in the unrolled state (Shen et al. 2009). The analytical results presented by Shen et al. (2009) show that internal forces in the tunnel lining are altered significantly due to the rolling correction operation during DOT construction. With the increase in the rolling correction angle, the magnitude of the internal forces changed remarkably. The internal force increased at some nodes and decreased at other nodes, leading to the change in its sign. To control the rolling within 0.6° of the DOT shield, the following measures were adopted (Shen et al. 2006; Bai and Tang 2007):

(1) *Control of rolling correction jacks* — This countermeasure is conducted by using rolling correction jacks at the circumference of the shield, to correct the rolling (RANSTT 1998; Ishihara et al. 2003).

(2) *Control of the soil conveyor* — Because the rotation speed of screw conveyors on each side of the tunnel can be controlled at different states, earth pressures acting on the two cutters can be adjusted to different values. Therefore, the torques of the two cutters are different. As a result, rolling can be corrected by using cutters with different torques (RANSTT 1998; Ishihara et al. 2003).

(3) *One-side loading* — This is a simplest way to correct rolling. When the level of one side is higher than the level of the other side, the weight of the elevated side is increased via control of three different bodies of the DOT shield in the following three ways (see Fig. 1): (*i*) leave a larger amount of soil in the soil chamber and on the screw conveyor at the elevated side by slowing the conveyor down; (*ii*) mount lead blocks in the middle body at the clearance between jacks; (*iii*) suspend segments in the tail body during shield jacking.

(4) *Overexcavation by the copy cutter* — To correct the rolling, some overexcavation can be carried out on the side opposite the rolling direction. Generally, this measure should be avoided because overexcavation will increase settlement (RANSTT 1998).

(5) *Real-time grouting* — If overexcavation is conducted, the volume of grouting should be increased to compensate for the overexcavated soil. Grouting will result in a rolling correction torque on the DOT shield.

(6) *Secondary grouting* — After the lining of the DOT is assembled, the rolled tunnel can also be corrected by use of secondary grouting in the opposite direction from the rolling. This method will produce a torque opposite to the rolling direction.

In addition, it is suggested that a highly precise apparatus must be employed to measure the tunnel direction, which can detect rolling at its earliest stage so that it can be corrected as soon as possible (RANSTT 1998; Yonei 2000).

Analytical method for one-side loading

Subsoil condition

The metro tunnel from Minsheng Road Station to North Yangjing Station of Shanghai Metro Line 6 is located at the Pudong New Development Area of Shanghai. It was constructed using a DOT shield. This DOT is 395 m long and consists of 329 segments, which are labeled consecutively from R1 to R329 (see Fig. 5). The tunnel was constructed in a very soft clay (MC) deposit at an elevation of approximately –3 to –12 m.

The elevation of the ground surface at the construction site is 3–5 m above sea level. The soft deposit of Shanghai is a multi-aquifer–aquitard system with a high groundwater

Fig. 5. Longitudinal section of DOT in Shanghai Metro Line 6. BF, backfill; MC, very soft clay; MSC, soft silty clay; SC, silty clay.

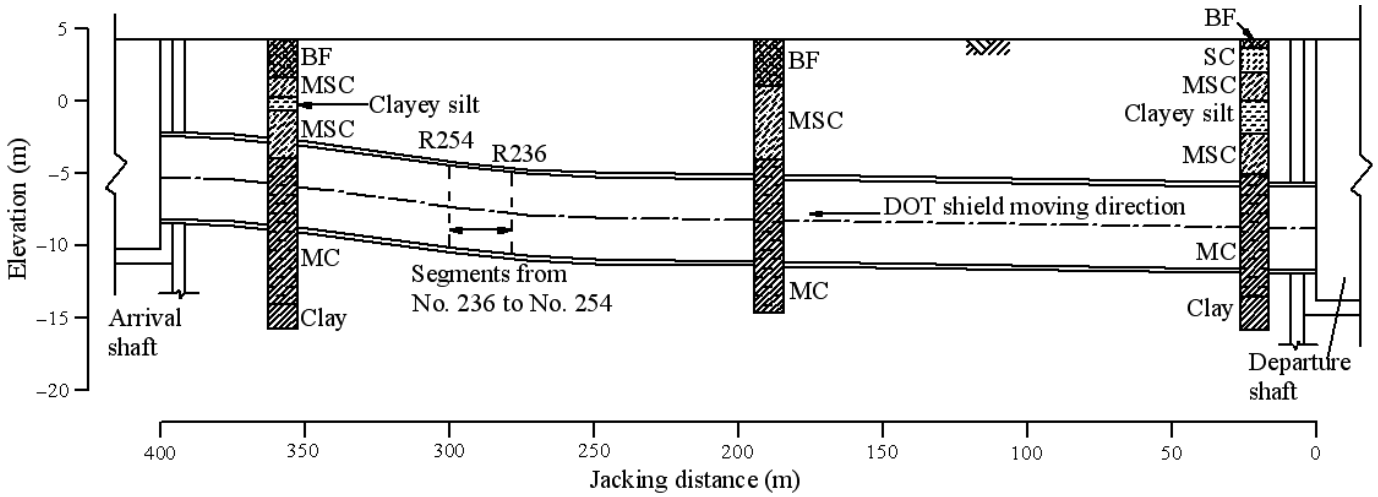

level (Xu et al. 2009). The groundwater level fluctuates between 1 and 2 m below the ground surface. Three boreholes were drilled to investigate the geological and geotechnical condition at the site (see Fig. 5). The first layer is loose backfill with a depth of 1–4 m. Under the fill layer, a sequence of layered soft soils with an overall thickness of over 10 m is present, including a silty clay (SC), a soft silty clay (MSC) with clayey silt lens, and MC. The soft soil is in a lightly overconsolidated state and is classified as clay (CL) based on the Unified Soil Classification System (ASTM 2006) method. The soft soil is underlain by medium to stiff SC layers from a depth of 17 to 30 m.

Figure 6 presents the geotechnical profile and soil properties of the subsoil at borehole BH-1. The grain-size distribution test on soil samples from borehole BH-1 indicates that this MC consists of clay, silt, and sand with a distribution 43%, 52.7%, and 4.3%, respectively. Water content is generally close to its liquid limit and the plasticity index of this MC is about 20%. The initial void ratio, e, was determined based on soil physical properties from laboratory tests. The compression index, C_c, was obtained from laboratory oedometer tests. Figure 7 shows the typical e–logP_c curves for each layer obtained from oedometer tests, where P_c is the consolidation pressure. The C_c value is about 0.15 for stiff clay. For MC, C_c varies from 0.4 to 0.75. From Fig. 7, it can be seen that the yield stress, P_y, varies from 80 to 450 kPa. The profile of the tip resistance from a cone penetration test and the sensitivity are also presented in Fig. 6. These results indicate that weak, compressible, and sensitive soils exist below an elevation of 13.2 m. The sensitivity of these soft clays ranges from 4.0 to 5.0.

Modeling methodology for one-side loading

Range of calculation

To evaluate the effectiveness of the rolling correction with one-side loading, FEM analysis under a two-dimensional (2D) condition was conducted. The reason for choosing the 2D condition is discussed in a later section. The modeled range is a 25 m depth from the ground surface and a 40 m horizontal distance from the DOT shield centerline. The diameter of the DOT shield is set as 6.2 m and the distance between the two centers is 4.6 m in the numerical analysis. The buried depth of the centerline of the shield is 12.5 m. Figure 8 shows the FEM model and calculation mesh for a DOT shield with a rolling angle, α, of 0.625°.

Loading approaches

As shown in Fig. 1, the width of the soil chamber is 0.915 m. In the head body, the maximum unbalanced one-side load is ~450 kN. In the tail body, one or two segments can be hung up by the segment assembling device, and the load is ~32–60 kN/m, distributed within the longitudinal loading length of 3.11 m. In the middle body, lead blocks are allocated as required within the available longitudinal length of 3.17 m. Therefore, the load along the longitudinal direction of the DOT shield is nonuniformly distributed, and the actual movement and loading condition of the DOT shield during construction is three-dimensional. In this study, a 2D plain strain condition is adopted to simulate the middle body of the shield under lead block loading. The reason for choosing 2D analysis is to simplify the problem, which is useful to illustrate the concept of one-side loading. Moreover, it is difficult to estimate soil weights in the DOT shield accurately, which may result in inaccuracy for three-dimensional modeling.

In construction, there are different load types, i.e.; distributed load, such as remaining soil; point load, such as suspended segments; or separately distributed lead blocks. Therefore, three types of load (i.e., one-point, four-point, and distributed) were adopted to simulate one-side loading. For a one-point load condition, a load was applied on the shell of the shield element at the node 1.5 m away from the shield center (see Fig. 9*a*). For the four-point load condition, loads were applied on the shield element with an even spacing of 0.5 m, and the first point was 0.75 m from the shield center (see Fig. 9*b*). For the distributed load condition, loads were uniformly applied on the shield element within the transverse length of 1.5 m, and the left edge was 0.75 m from the shield center (see Fig. 9*c*). The magnitude of the one-point load was from 0 to 380 kN/m. The resulting magnitude and position for the case of the four-point load and the case of the distributed load were the same as those for the case of the one-point load. Therefore, the magnitude for

Fig. 6. Soil profile and properties at the construction site. q_s, cone tip resistance; S_t, sensitivity; w_L, liquid limit; w_n, natural water content, w_p, plastic limit; γ_t, unit weight.

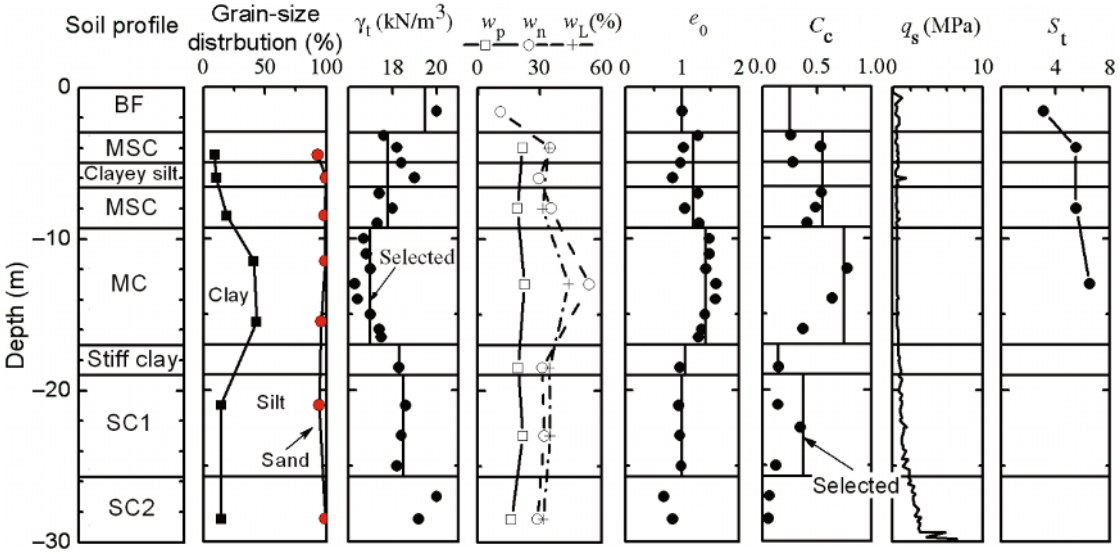

Fig. 7. Typical e–logP_c curves for each layer from oedometer tests.

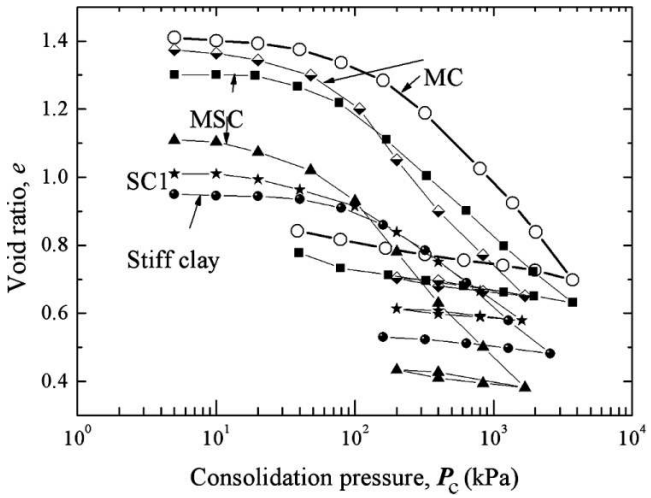

each point of the four-point load condition was calculated to be 0–95 kN/m. The calculated resultant and the intensity of the distributed load are from 0 to 380 kN/m and 0 to 253.3 kN/m/m, respectively. Moreover, the mesh around the DOT shield was refined in FEM analysis. For the one-point load condition, as it may have resulted in a loading concentration phenomenon, an artificial densification for the shell element and node on which loading was applied was conducted in the numerical analysis.

Initial and boundary conditions

In the model, the DOT shield was initially assumed to be in a rolling state with several selected rolling angles and vertical differences of horizontal levels between the two centerlines, as shown in Table 1. Groundwater was set at 1.5 m below the ground surface. Displacement boundary conditions were set as follows: inside the lining, there was a free boundary; at the bottom, both vertical and horizontal displacements were constrained; for the left and right vertical boundaries, the horizontal displacement was constrained. Each boundary was modeled under drained conditions.

Materials and parameters

As shown in Fig. 6, physical and mechanical properties of the three layers (MSC, clayey silt, and MSC) under the top crust are similar. In an FEM calculation, the soft subsoil was divided into five layers, i.e., backfill, MSC, MC, stiff clay, and SC. Parameters of these soft soils are tabulated in Tables 2 and 3. The mechanical behavior of subsoils was represented by the soft soil model as shown in the Plaxis package (Brinkgreve 2004). Model parameters for each layer are listed in Table 2. The modified compression index, λ^*, and the modified swelling index, κ^*, were derived from C_c and the swelling index, C_r, as shown in the following equations (Brinkgreve 2004):

$$[1] \qquad \lambda^* = \frac{C_c}{2.3(1+e)}, \qquad \kappa^* = \frac{2}{2.3}\frac{C_r}{1+e}$$

Values of C_c and C_r were determined from oedometer tests, as shown in Figs. 6 and 7. However, as shown in Fig. 6, C_c is very scattered for each layer, which is mainly due to the effect of sampling disturbance (Hong and Han 2007). Laboratory tests show that the average value of C_c for remolded samples of the MC layer in Shanghai is about 0.3 (Zhou and Sun 2009). It is thought that C_c for the in situ MC must be higher than 0.3. Therefore, the highest value of C_c for each layer was adopted in the FEM analysis, shown as the selected vertical lines in Fig. 6.

The critical state ratio, M, was derived from triaxial compression tests (Su 1979; Huang and Gao 2005), as shown in Fig. 10. In the Plaxis package, the critical state ratio, M, is determined approximately from the following equation (Brinkgreve 1994):

$$[2] \qquad M = 3.0 - 2.8K_0$$

where K_0 is the lateral earth pressure coefficient at rest.

The subsoil is in a lightly overconsolidated state for the

Fig. 8. Calculation model for DOT shield rolling correction using the one-side loading method: (*a*) mesh and boundary condition; (*b*) rolling state of DOT shield.

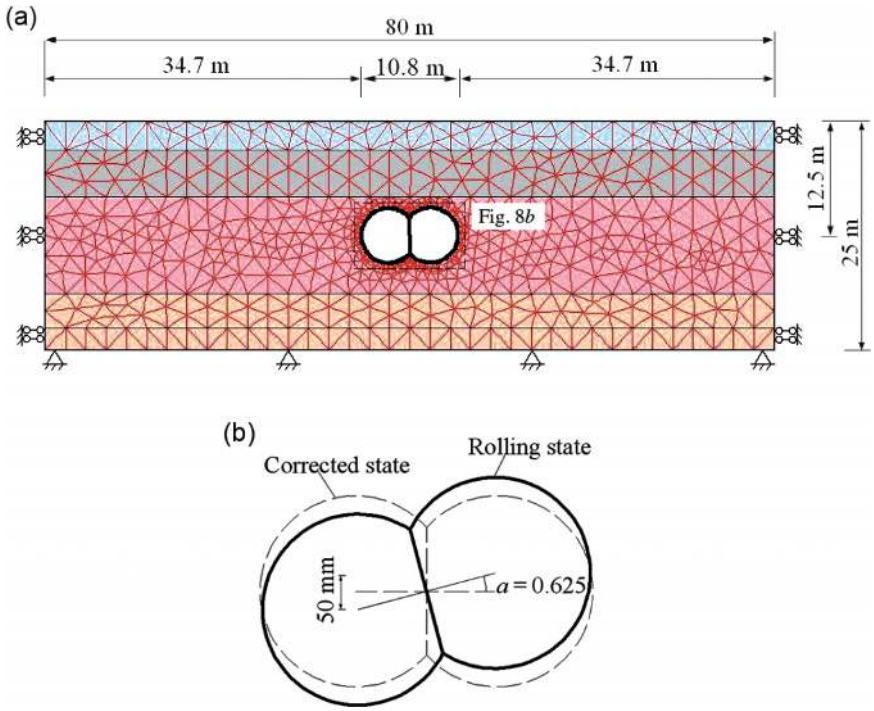

Fig. 9. Position of load applied on the DOT shield: (*a*) one-point load; (*b*) four-point load; (*c*) distributed load.

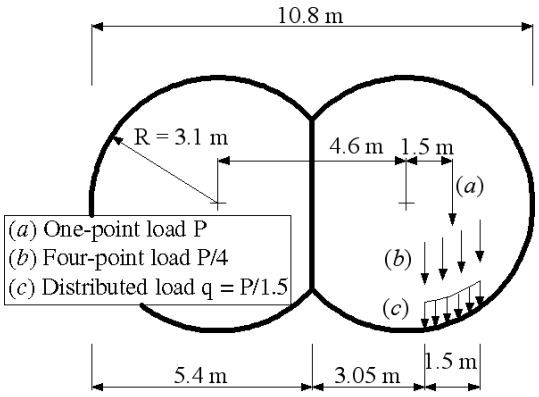

Table 1. Initial rolling angle versus vertical difference of horizontal levels between two centerlines in FEM analysis.

Difference between two centerlines (mm)	Rolling angle (°)
10	0.125
20	0.250
30	0.375
40	0.500
50	0.625
100	1.250
150	1.875
200	2.500
250	3.125

soft layers; however, the top crust layer is in a highly overconsolidated state with an overconsolidation ratio, OCR, of about 6. The values of K_0 were calculated using the equation proposed by Mayne and Kulhawy (1982)

$$[3] \qquad K_0 = (1 - \sin\phi')(\mathrm{OCR})^{\sin\phi'}$$

where ϕ' is the effective friction angle of the soil.

Using eqs. [2] and [3], calculated parameters for each soil layer are tabulated in Table 3. The initial stress in the FEM calculation was derived from K_0. Poisson's ratio, ν, for the subsoil was selected based on experience. The shield material was assumed to be an elastic material, with an axial stiffness, EI = 1.4×10^8 kN/m, and a flexural rigidity, EA = 1.43×10^6 kN·m^2/m. The equivalent thickness of the shell was assumed to be 0.1 m and the weight was assumed to be 8.4 kN/m/m. Poisson's ratio for the DOT shield material was 0.15.

Results and discussion

Relation between rolling angle and correction load

Figure 11 shows the variation in rolling correcting load with different initially assumed rolling angles, and illustrates the calculated results for the one-point, four-point, and distributed load cases. The intersection of the horizontal axis and the curve represents the initially assumed rolling angle. From this figure, the required correction load can be determined for a given rolling angle. Rolling angle decreases with an increase in one-side load. For point load cases, when the initial rolling angle is small, the relation between correction load and angle is approximately linear. The relation becomes nonlinear when the initial rolling angle is large, indicating that the soil under the DOT shield has

Table 2. Input parameters of each soil layer used in FEM analysis.

Soil layer	Thickness (m)	γ_t (kN/m^3)	e_0	ν	κ^*	λ^*
Backfill	3.2	20.0	1.0	0.3	0.030	0.054
Soft silty clay	5.9	17.8	1.3	0.3	0.013	0.109
Soft clay	8.6	17.2	1.4	0.3	0.050	0.130
Stiff clay	2.7	18.1	1.1	0.3	0.018	0.031
Silty clay	3.4	18.3	0.9	0.3	0.032	0.087

Note: e_0, initial void ratio; ν, Poisson's ratio.

Table 3. Derived values of the lateral earth pressure coefficient at rest, K_0; critical state ratio, M; and other parameters for each soil layer.

Soil layer	Thickness (m)	γ_t (kN/m^3)	ϕ' (°)	OCR	K_0	M
Backfill	3.2	20.0	35	3	0.80	0.8
Soft silty clay	5.9	17.8	32	1.5	0.68	1.0
Soft clay	8.6	17.2	25	1.5	0.61	1.3
Stiff clay	2.7	18.1	35	2.0	0.63	1.2
Silty clay	3.4	18.3	30	1.5	0.61	1.3

Note: OCR, overconsolidation ratio; ϕ', effective frictional angle.

Fig. 10. Overconsolidation ratio (OCR), yield stress (P_y), and effective frictional angle (ϕ') from triaxial tests (based on Huang and Gao 2005). σ'_{v0}, in situ vertical effective stress.

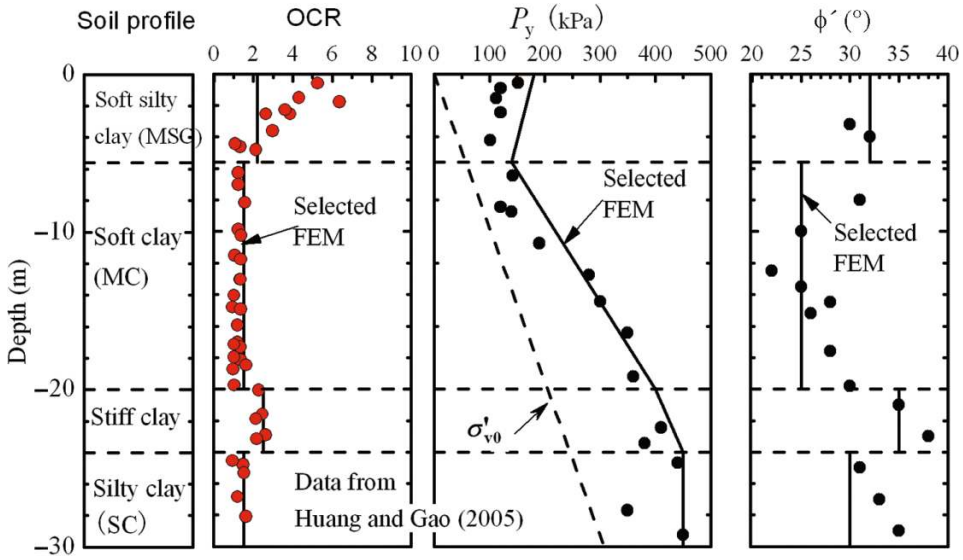

been in a plastic state under a large load. In engineering practice, Fig. 11 can be used, through interpolation, as a design chart for a given initial rolling angle.

Figure 12 presents the relationship between initially assumed rolling angle and the required perfect correcting load, P. Theoretically, the perfect correcting load is defined as the load that is required to correct the rolling angle to zero. The slope of the curves becomes gentle at high rolling angle (e.g., larger than 1.0°). From Figs. 11 and 12, for a given initial rolling angle, there is no considerable difference in the required correcting load among the one-point, four-point, and distributed loads. The difference between the one-point and four-point load conditions is less than 4%, and the difference between the four-point and distributed load conditions is less than 2%. As the moment with respect to the centerline of the DOT for these three loading patterns is the same, the difference is thought to be caused by the loading concentration. Therefore, the multi-point load or distributed load pattern is more reasonable than the one-point load pattern in the FEM analysis.

Relation between surface settlement and rolling angle

The settlement induced by shield tunneling is due to ground loss during excavation (Peck 1969*a*). There are many proposed methods to predict short-term (during construction) and long-term (consolidation) settlement, e.g., an empirical equation (Peck 1969*a*) based on observation (Peck 1969*b*), FEM analysis based on the "gap parameter" (Lee and Rowe 1991; Lee et al. 1992), and analytical solutions (Chou and Bobet 2002; Park 2004). The settlement mechanism was also investigated using centrifuge modeling (Nomoto et al. 1999). Liao et al. (2008) presented an analysis of the surface settlement induced by long-term longitudinal stress transfer.

Rolling control will inevitably disturb soils surrounding the DOT shield and result in a certain loss of subsoil due to

Fig. 11. Calculated correcting load versus initially assumed rolling angle for one-point, four-point, and distributed loads.

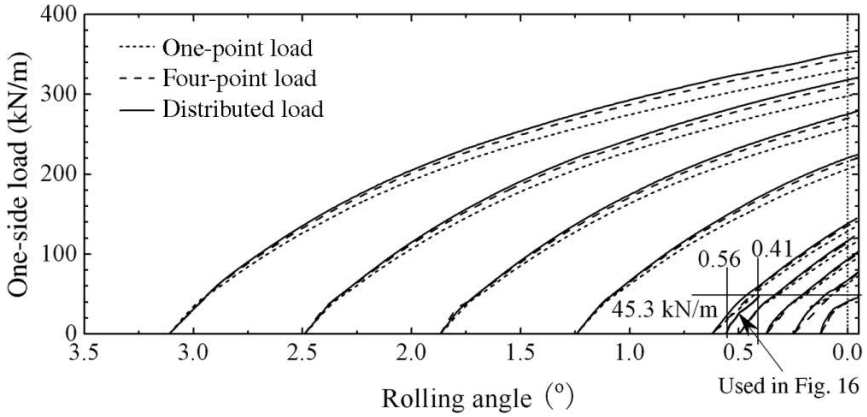

Fig. 12. Initial rolling angle versus calculated perfect correcting load required to correct the rolling angle to zero theoretically.

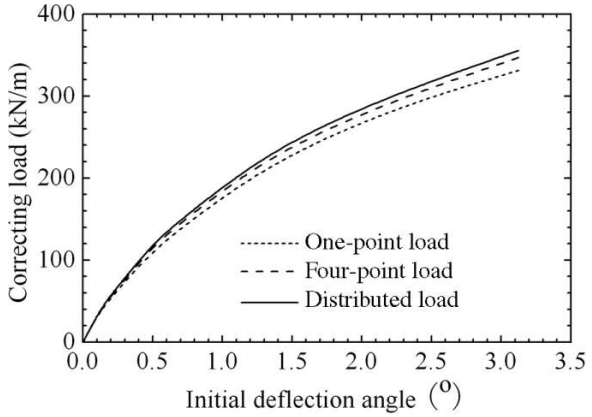

Fig. 13. Initial rolling angle versus maximum settlement due to rolling correction.

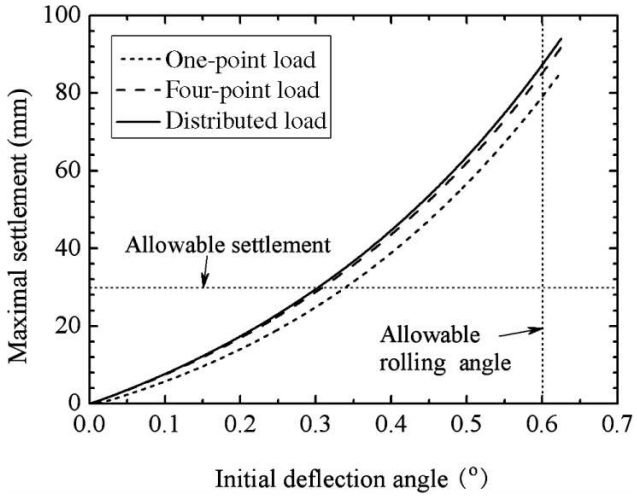

overexcavation by copy cutters, which will induce surface settlement. A one-side load would disturb surrounding soil and cause excess settlement. Consequently, it is necessary to calculate the surface settlement over the tunnel induced by the rolling correction operation. In engineering practice, the volume of tail grout is generally increased to compensate for this surface settlement (RANSTT 1998). The Shanghai Metro Line 8 tunnel was constructed using the DOT shield method. The volume of injected tail grout in Shanghai Metro Line 8 reached 2.5 times the gap volume between the shield and tunnel (Bai and Ding 2008), which indicates that most of the tail grout was used to compensate for the ground loss induced by other construction factors, e.g., rolling correction rather than the gap.

Figure 13 presents the relationship between the initially assumed rolling angle and the maximum surface settlement due to rolling correction. From this figure, it can be found that with an increase in the rolling angle, settlement increases. When the rolling angle is larger than 0.3°, the induced settlement exceeds the allowable value. For the allowable rolling angle of 0.6°, the corresponding settlement is 85 mm, which is far beyond the allowable limit.

Figure 14 shows the surface settlement trough caused by the operation of the rolling correction. As shown in the figure, the transverse settlement curve is asymmetric. Consequently, some other measures such as real-time grouting should be carried out during rolling correct operation with one-side loading. In particular, increasing grouting volume at the uplifted side is useful for deformation control.

Fig. 14. Calculated transverse surface settlement trough due to rolling correction. IRA, initial rolling angle.

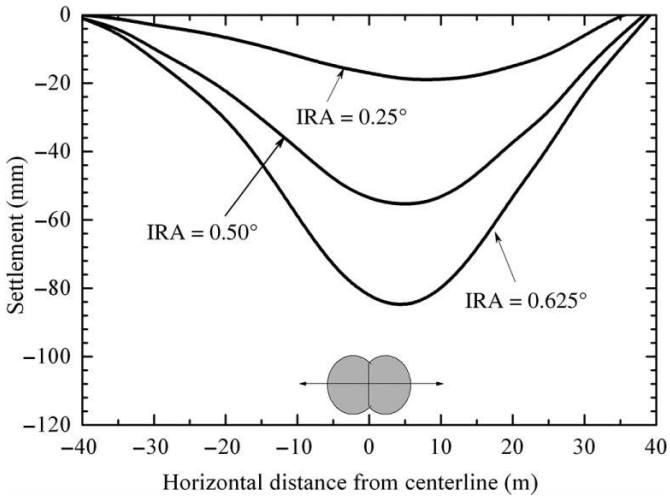

Fig. 15. Field-observed rolling curve during rolling correcting operations.

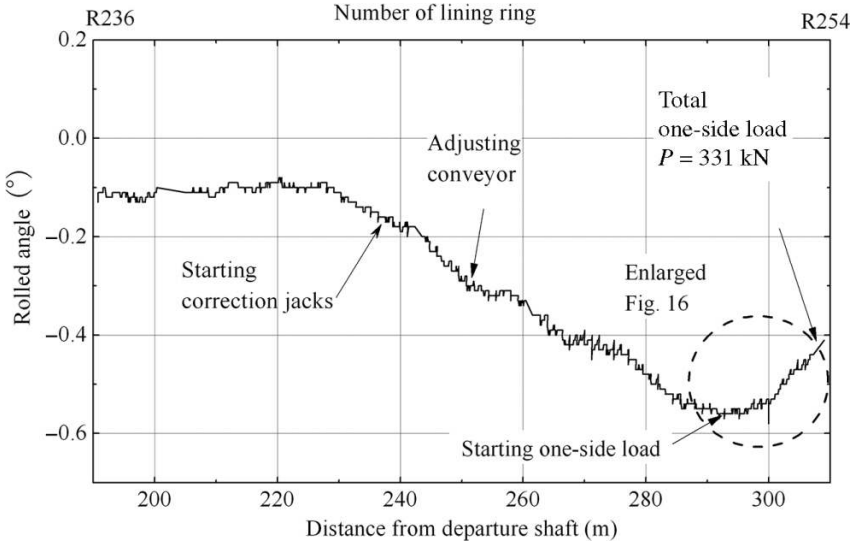

Verification based on field observation

Field experience (Shen et al. 2006) showed that to restrict the rolling angle to the range of allowable values, when the rolling angle reaches some selected value, i.e., 0.2°, the rolling correction operation is generally conducted in the following sequence: start rolling correction jacks, adjust the excavated soil volume with the screw conveyor, apply block loading at one side, and increase grouting volume. If these measures are not effective, overexcavation using a copy cutter can be subsequently conducted.

In Shanghai Metro Line 6, there was an upward slope located in the MC layer (see Fig. 5), where rolling occurs easily. Figure 15 presents the field-observed rolling curve during rolling correcting operations. The negative rolling angle presented in Fig. 15 represents the clockwise direction. Recording of the rolling angle was started when the DOT shield was launched. When the rolling angle reached 0.18° (235 m from launching shaft), the rolling correction operation was started with jacks at first. However, rollingdeveloped continuously until 0.30° (250 m). For this reason, the speed of the screw conveyor at the elevated side was reduced to maintain more excavated soils at this side, which was about 149 kN heavier than at the depressed side. The rolling angle was set to 0.30° within eight rings (250–260 m). Once the jacked distance reached ~260 m from the launching shaft, the rolling angle increased again. This phenomenon indicates that the adjustment of the soil conveyor speed had begun to lose its effectiveness. The rolling angle continued to increase until it reached a temporary state, i.e., 0.41° within 10 rings (from 265 to 277 m). However, after 277 m, rolling developed again. This observation shows that all of the aforementioned rolling correcting measures were not sufficient. Therefore, one-side loading with lead blocks was adopted when the rolling angle reached 0.56° (292 m). The lead block was gradually added from 0 to 150 kN within 17 m (292 to 309 m). At the same time, a segment with a 32 kN weight was attached with the hook of the assembling device. It was found that with these two measures, the rolling angle decreased considerably (Fig. 15). The recorded rolled angle decreased to 0.41° (309 m). Compared with the recorded maximum rolling angle (0.56°), the corrected rolling angle reached 0.14° within the distance of 309 m. In other words, 25% of the maximum rolling angle had been corrected using the one-side load method, indicating that one-side loading is very effective in controlling rolling.

Figure 16 illustrates a comparison between the observed and calculated rolling angles during correction operation via one-side loading. Here, it must be mentioned that the calculated value was not calculated directly from FEM; it was done through the following procedure. Figure 11 was employed to derive the one-side load value of 45.3 kN/m by interpolation, indicating that the rolling angle was corrected from 0.56° initially to 0.41° (0.14° change). This load was gradually applied during the construction of 14 lining rings, and for each ring the average corrected rolling angle was calculated as 0.01°. Therefore, the correcting load was ~3.24 kN/m per ring, and a one-side load of about 326 kN was required along the longitudinal shield length (~7.195 m). As the balance soil in the soil chamber was 149 kN and the suspended segment was 32 kN, the required lead block weight was then theoretically calculated as about 141 kN based on force equilibrium. This value is slightly smaller than the field value, 150 kN, as illustrated in Fig. 16. The calculated rolling angle changed from 0.56° to 0.41° within 17 m, which is easily consistent with the field-observed value. It is therefore concluded that the calculated result is applicable in engineering practice.

Conclusions

One-side loading is one of the countermeasures used to correct the rolling of DOT shields during construction. This paper presents an FEM simulation of the one-side loading procedure in rolling correction of DOT shields. The following conclusions can be drawn:

(1) With an increase in one-side loading, the rolled angle can be reduced indicating that one-side loading is a cost-effective rolling correction method.

(2) Under one-side loading, plastic deformation of the soil

Fig. 16. Variation of rolling angle upon one-side load versus jacked distance.

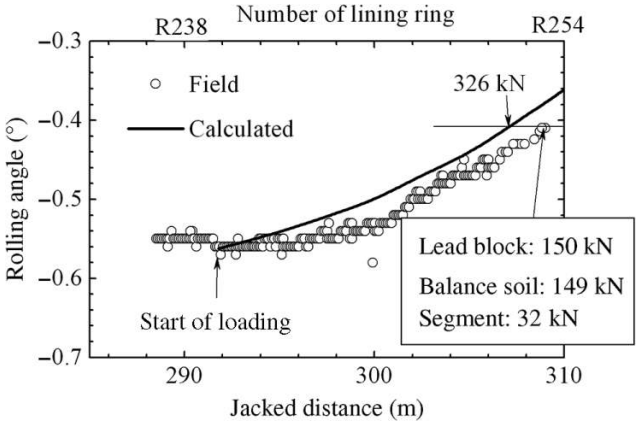

below the shield occurred when the loading was very large. Therefore, one-side loading should be applied step by step.

(3) In the Shanghai soft deposit, at the allowable rolling angle, the corresponding maximum surface settlement due to the rolling correction greatly exceeds the allowable settlement. Therefore, the grouting volume should be increased to reduce rolling correction–induced settlement.

(4) Field observation on the process of rolling correction with one-side loading during the construction of the DOT of Shanghai Metro Line 6 was monitored. The FEM result is compared with the field-observed data. It is found that the FEM result can predict the field data well.

(5) The FEM result shows that rolling correction operation could cause asymmetrical distribution of the surface settlement trough and additional internal forces in tunnel linings. Therefore, rolling should be corrected when the rolling angle is still very small.

Acknowledgements

The research work described herein was funded by the National Nature Science Foundation of China (NSFC, Grant No.50779035) and the joint research program between NSFC and the Japan Society for the Promotion of Science (JSPS) (Grant No. 50911140105). It was also supported by the Shanghai Leading Academic Discipline Project (Project No. B208). This financial support is gratefully acknowledged. The authors would like to express their appreciation to Mr. T. Ueno (Maeda Construction Co. Ltd., Japan) for his suggestions concerning the fieldwork, and are also grateful to the anonymous reviewers whose constructive comments helped improve the quality of this paper.

References

ASTM. 2006. Standard practice for classification of soils for engineering purposes (Unified Soil Classification System). ASTM standard D2487. American Society for Testing and Materials, West Conshohocken, Pa.

Bai, Y., and Ding, Z.C. 2008. Construction technology of tunneling boring machine. China Architecture and Building Press, Beijing, China. 320p. [In Chinese.]

Bai, Y., and Tang, J. 2007. Experience and lessons from underground construction in Shanghai. China Civil Engineering Journal, **40**(5): 105–110. [In Chinese.]

Brinkgreve, R.B.J. 1994. Geomaterial models and numerical analysis of softening. Ph.D. dissertation, Delft University of Technology, Delft, the Netherlands.

Brinkgreve, R.B.J. 2004. PLAXIS-2D — user's manual and scientific manual. Version 8 [computer program]. A.A. Balkema, Rotterdam, the Netherlands.

Chou, W.I., and Bobet, A. 2002. Predictions of ground deformations in shallow tunnels in clay. Tunnelling and Underground Space Technology, **17**(1): 3–19. doi:10.1016/S0886-7798(01)00068-2.

Hong, Z., and Han, J. 2007. Evaluation of sample quality of sensitive clay using intrinsic compression concept. Journal of Geotechnical and Geoenvironmental Engineering, **133**(1): 83–90. doi:10.1061/(ASCE)1090-0241(2007)133:1(83).

Huang, S.M., and Gao, D.Z. 2005. Foundation and underground engineering in soft ground. China Architecture and Building Press, Beijing. [In Chinese.]

Iida, H., and Sumida, M. 1992. Construction of first DOT tunnel in Japan. Tunnels and Underground, **23**(6): 7–12. [In Japanese.]

Ishihara, S., Harada, S., and Hayamizu, M. 2003. Control of moving trajectory of DOT shield and nearby construction through existing pile for the tunnel of Nagoya Express Railway No. 4. Tunnels and Underground, **34**(7): 35–43. [In Japanese.]

Lee, K.M., and Rowe, R.K. 1991. An analysis of three-dimensional ground movements: the Thunder Bay tunnel. Canadian Geotechnical Journal, **28**(1): 25–41. doi:10.1139/t91-004.

Lee, K.M., Rowe, R.K., and Lo, K.Y. 1992. Subsidence owing to tunnelling. Part I. Estimating the gap parameter. Canadian Geotechnical Journal, **29**(6): 929–940. doi:10.1139/t92-104.

Liao, S.M., Peng, F.L., and Shen, S.L. 2008. Analysis of shearing effect on tunnel induced by load transfer along longitudinal direction. Tunnelling and Underground Space Technology, **23**(4): 421–430. doi:10.1016/j.tust.2007.07.001.

Mayne, P.W., and Kulhawy, F.H. 1982. K_0-OCR relationships in soils. Journal of Geotechnical Engineering, **108**(GT6): 851–872.

Nomoto, T., Imamura, S., Hagiwara, T., Kusakabe, O., and Fujii, N. 1999. Shield tunnel construction in centrifuge. Journal of Geotechnical and Geoenvironmental Engineering, **125**(4): 289–300. doi:10.1061/(ASCE)1090-0241(1999)125:4(289).

Park, K.H. 2004. Elastic solution for tunneling-induced ground movements in clays. International Journal of Geomechanics, **4**(4): 310–318. doi:10.1061/(ASCE)1532-3641(2004)4:4(310).

Peck, R.B. 1969*a*. Deep excavations and tunneling in soft ground: State-of-the-art report. *In* Proceedings of the 7th International Conference on Soil Mechanics and Foundation Engineering, Mexico City, Mexico, 25–29 August 1969. pp. 225–290.

Peck, R.B. 1969*b*. Advantages and limitations of the observational method in applied soil mechanics. Géotechnique, **19**(2): 171–187. doi:10.1680/geot.1969.19.2.171.

RANSTT. 1998. New shield tunneling technology. Civil Engineering Press, Tokyo. [In Japanese.]

Shen, S.L., Cai, F.X., Bai, T.H., and Zhu, J.M. 2006. Direction deviation control during Double-O-Tube (DOT) tunnel construction. *In* Underground Construction and Ground Movement. Geotechnical Special Publication No. 155. *Edited by* H. Zhu, F. Zhang, E.C. Drumm, C.T. Chin, and D. Zhang. American Society of Civil Engineers (ASCE) Press, Reston, Va. pp. 185–192.

Shen, S.-L., Horpibulsuk, S., Liao, S.M., and Peng, F.-L. 2009. Analysis of the behavior of DOT tunnel lining caused by rolling correction operation. Tunnelling and Underground Space Technology, **24**(1): 84–90. doi:10.1016/j.tust.2008.05.003.

Su, H.Y. 1979. Investigation on the deformation characteristics of

soft deposit in Shanghai under pumping and recharge. Chinese Journal of Geotechnical Engineering, **1**(1): 24–35. [In Chinese.]

Xu, Y.-S., Shen, S.-L., and Du, Y.-J. 2009. Geological and hydrogeological environment in Shanghai with geohazards to construction and maintenance of infrastructures. Engineering Geology, **109**(3–4): 241–254. doi:10.1016/j.enggeo.2009.08.009.

Yonei, Y. 2000. Construction of common underground municipal facility using large diameter DOT shield. *In* Construction Technology Shield Tunnel. *Edited by* A. Koyama, K. Ohishi, and T. Noguchi. Civil Engineering Press, Tokyo. pp. 190–197. [In Japanese.]

Zhou, K., and Sun, D.A. 2009. Experiments on compression characteristics of remoulded soft clay in Shanghai. Journal of Shanghai University (Natural Science Edition), **15**(1): 99–104.